

## A new concept in modeling the dielectric response of sandstones: Defining a wetted rock and bulk water system

Rosemary Knight\* and Anthony Endres‡

### ABSTRACT

Experimental data for the real part of the dielectric constant ( $K'$ ) of three sandstone samples are considered as a function of the level of water saturation ( $S_w$ ) in the frequency range 60 kHz to 4 MHz. Existing theoretical models have previously shown poor agreement with  $K'$  versus  $S_w$  data for rock samples, undoubtedly due to the complexity involved in adequately accounting for geometrical and electrochemical effects. In analyzing the data presented here, we find a pronounced increase in  $K'$  in the low saturation region which in all cases can be attributed to the establishment of geometrical and surface effects associated with the rock-water interface. When this increase in  $K'$  is accounted for by defining wetted matrix parameters, the data show excellent agreement with existing theoretical models.

### INTRODUCTION

Calculating the dielectric constant of a composite material has been an active topic of research for many years in various fields of study. The dielectric constant of a material is a complicated product of the individual dielectric constants of the various components, the volume fractions of the components, the geometries of the components, and the electrochemical interactions among the components. The complex dielectric constant  $K^*$  can be written as

$$K^* = K' - iK''$$

where  $K'$  is the real part and  $K''$  is the imaginary part of the complex dielectric constant. Of particular interest in this work is the problem of theoretically calculating  $K'$  of a porous rock sample containing various amounts of water. This is of great practical interest, because the measurement of  $K'$  in both petroleum exploration and groundwater inves-

tigations can be potentially very useful in determining the level of water saturation.

A number of theoretical methods have been proposed to determine the dielectric constant of water-saturated rock. One approach involves using simple mixing laws to calculate the total dielectric constant of the material ( $K^*$ ), given only the dielectric constant ( $K_i^*$ ) and the volume fraction ( $V_i$ ) of each of the  $i$  components. One such mixing law, the complex refractive index method (CRIM) (Wharton et al., 1980), is commonly used in interpreting dielectric measurements made in oil and gas wells:

$$\sqrt{K^*} = \sum_i V_i \sqrt{K_i^*}$$

This expression can be expanded for the case of a rock at some level of water saturation  $S_w$ , where  $S_w$  is the volume fraction of the pore space filled with water, the remainder being filled with hydrocarbon. The system is composed of dry rock ( $r$ ), water ( $w$ ), and hydrocarbon ( $h$ ), with porosity  $\phi$ ;  $K^*$  is given by the following expression:

$$\sqrt{K^*} = (1 - \phi)\sqrt{K'_r} + S_w\phi\sqrt{K'_w} + (1 - S_w)\phi\sqrt{K'_h}$$

The dielectric constants of the rock and the hydrocarbon are treated as real, not complex, because these components are assumed to be insulating (i.e.,  $K'' = 0$ ). An obvious limitation of this method is that it does not take into account the geometry of the components or electrochemical interactions among components.

As an alternate approach to calculating  $K'$ , Feng and Sen (1985) used a form of the differential effective medium approximation (Norris et al., 1985) to derive an expression for the dielectric properties of a partially saturated rock. By assuming that the rock matrix and hydrocarbon exist as spherical inclusions in a water-brine background, and that the rock matrix and hydrocarbon are perfect insulators, the following differential form is obtained:

Manuscript received by the Editor January 13, 1989; revised manuscript received September 27, 1989.

\*Department of Geological Sciences, University of British Columbia, Vancouver, B.C., Canada V6T 2B4.

‡Department of Geophysics and Astronomy, University of British Columbia, Vancouver, B.C., Canada V6T 1W5.

© 1990 Society of Exploration Geophysicists. All rights reserved.

$$\frac{dK^*}{3K^*} = \frac{dV_m}{V_m + V_w + V_n} \frac{K'_m - K^*}{K'_m + 2K^*} + \frac{dV_n}{V_m + V_w + V_n} \frac{K'_n - K^*}{K'_n + 2K^*}$$

[equation (2), Feng and Sen, 1985], where subscripts  $m$ ,  $w$ , and  $n$  refer to matrix, water, and hydrocarbon, respectively. In solving this expression, it was assumed that  $dV_m$  and  $dV_n$  were related by

$$\frac{dV_m}{dV_n} = \frac{(1 - S_w)\phi}{(1 - \phi)}$$

and the initial value problem was solved. The analytic expression for the solution of this problem is given by Feng and Sen [1985, equation (3)]. In this derivation neither complicated geometrical effects nor electrochemical effects were considered.

It has been clearly shown experimentally that the geometry of components in a porous rock containing water and/or hydrocarbons can have a large effect on  $K'$  (Sen, 1980; Kenyon, 1984; Knight and Nur, 1987a, b). These geometrical effects have been included in theoretical models by defining parameters to account for the shapes and/or distribution of shapes of the components (Sen, 1980; Lysne, 1983; Kenyon, 1984; Feng and Sen, 1985; Sherman, 1987). In addition to geometry, it has been found that surface effects—the screening of charges and charge accumulation at interfaces within a rock—can contribute to the dielectric response of rocks (Keller and Licastro, 1959; Fuller and Ward, 1970; Sen, 1980). Despite such advances in our understanding of the dielectric mechanisms in rocks, there has been little success in modeling the dielectric response of a partially saturated rock sample over a wide range of saturations. The poor results are undoubtedly due to the complexities involved in incorporating both geometrical and surface effects in a model that includes variation in water saturation. Until now it has been unclear how geometrical and surface effects are related to the level of water saturation in a sample.

We have found a surprisingly simple way to account for geometrical and surface effects in the dielectric response of a rock containing water. The explanation is based on the observation that the magnitudes of all geometrical and surface effects are established once a rock-water interface exists in the sample, i.e., once the rock has been “wetted.” To model the dielectric response of a rock-water mixture, we redefine the basic components. Instead of “mixing” the dielectric response of *dry* rock and water to predict the dielectric response of water saturated rocks, as has always

been done, we mix the dielectric responses of the *wetted* rock and water.

This approach is analogous to the treatment of the problem of predicting saturated elastic wave velocities for rocks from the unsaturated values suggested by Gassmann (1951). In Gassmann's derivation, he clearly states that the saturated velocities cannot be predicted by starting with measured values for a totally dry rock, but by starting with elastic properties measured for a wetted rock, i.e., “adsorbed water has to be considered as part of the framework” (translated from Gassmann, 1951). We show here that the same is true for modeling the dielectric response of water-saturated rocks: the interaction between the rock and water, which can result in both geometrical and surface effects, can be included in any model by defining as a basic parameter the dielectric response of the rock wetted by, or in equilibrium with, the water.

In this paper we apply the idea of defining a wetted rock-bulk water system to model experimental measurements of  $K'$  as a function of  $S_w$  for three sandstones. With a high density of data, it is possible to identify and isolate geometrical and/or surface factors associated with the interaction between the rock and the water. Once these effects have been accounted for by using wetted matrix parameters in modeling the data, it is possible to obtain good agreement between experimental data and existing theories.

## EXPERIMENTAL RESULTS

We have considered dielectric data from three sandstone samples: CH61-79, CH58-79, and Berea 100. Descriptions of these sandstone samples are given in Table 1. The petrography was determined by thin-section analysis and taken from the Stanford Rock Physics catalog. Porosity was measured with a helium porosimeter. The surface areas were determined using a nitrogen adsorption technique.

The samples were prepared for dielectric measurements as thin disks, 5 cm in diameter and approximately .5 cm thick, with platinum electrodes sputtered on the two opposite flat faces of the disk. The measurements were made with a Hewlett-Packard 4192A impedance analyzer over the frequency range of 60 kHz to 4 MHz; details of the measurement procedure are given in Knight and Nur (1987a). The level of water saturation in a sample was determined by weighing the sample. Each sample was fully water saturated with deionized water then dried with dielectric measurements made as the sample dried. At low levels of water

Table 1. Sample Description.

Sample	$\Phi$	Petrographic description (as % total)								
		$S$ (m <sup>2</sup> /g)	S/V (cm <sup>-1</sup> )	Framework grains				Cements		
				Quartz	Chert	Feldspar	Lithics	Quartz	Clay	Carbonates
CH61-79	.070	2.97	$1.04 \times 10^6$	38	16	1	4(a)	16	3	15
CH58-79	.069	2.07	$7.38 \times 10^5$	30	12	—	6	—	18	18
Berea 100	.197	1.234	$1.33 \times 10^5$	53	2	3	8	11	7(b)	7

$\Phi$  = porosity, (a) argillaceous, (b) clay percentage includes minor chlorite and/or sericite.

saturation, data were also obtained by starting with a vacuum-dry sample and exposing it to room humidity.

The dielectric data from the three samples are shown in Figures 1a, 1b, and 1c. Data for two of the samples, CH61-79 and Berea 100, at different frequencies have been published previously (Knight and Nur, 1987a, b). In each figure  $K'$  is plotted as a function of  $S_w$  at 105 kHz and 1.2 MHz.  $S_w$  is the volume fraction of the pore space filled with water, the remainder being filled with air. The dominant form of the dependence of  $K'$  on  $S_w$  is similar for all the samples (and for all other frequencies in the measured range of 60 kHz to 4 MHz):  $K'$  increases rapidly with increasing  $S_w$  at low levels of  $S_w$  up to some critical saturation point  $S_w^0$ , beyond which  $K'$  increases more gradually and approximately linearly with increasing  $S_w$ . The magnitude of the increase at low saturations is frequency-dependent, increasing with decreasing frequency. Above  $S_w^0$  the slope of  $K'$  versus  $S_w$  varies between samples but is the same at all frequencies for any given sample. These are all critical aspects of the dependence of  $K'$  on  $S_w$  that must be considered in modeling the data.

The behavior of  $K'$  in the saturation region  $0 < S_w < S_w^0$  has been discussed in Knight and Nur (1987a, b) and attributed to effects associated with the presence of a thin layer of water coating the surface of the pore space. Referring to the experimental results presented here, it is possible to determine the apparent thickness of the surface water corresponding to the surface water effect. The  $S/V_{\text{pore space}}$  of each of the samples is given in Table 1. Using  $3.5\text{\AA}$  as the thickness of a monolayer of water (Thorp, 1959),  $S_w$  at low saturations can be converted to the number of completed monolayers; this conversion assumes that water covers the surface in uniform monolayers, a simplifying but reasonable assumption. In Figures 2a and 2b, the 105 kHz data from two of the samples, CH61-79 and CH58-79, are presented at low saturations as  $K'$  versus the number of completed monolayers. It is apparent from these figures that  $S_w^0$  corresponds to a surface coating of water three to four monolayers, or approximately 1 nm, thick. A second feature in these figures, the lack of change in  $K'$  with the first monolayer adsorbed, is due to the reduced  $K'$  for bound water, as discussed in Knight and Nur (1987b).

Once the surface of the pore space has been coated with approximately 1 nm of water, a large increase has occurred in  $K'$  of the rock-water system. The magnitude of  $K'$  at this saturation increases for any given sample with decreasing frequency, and between samples with increasing surface-area-to-volume ratio. In a sample with a higher  $S/V_{\text{pore space}}$ , the surface effect extends to higher levels of  $S_w$  and causes a greater magnitude of the measured value of  $K'$ . The increase in  $K'$  can be seen by comparing the data in Figure 1a for CH61-79 ( $S/V_{\text{pore space}} = 1.04 \times 10^6 \text{ cm}^{-1}$ ) with the data in Figure 1c for Berea 100 ( $S/V_{\text{pore space}} = 1.33 \times 10^5 \text{ cm}^{-1}$ ). In the data for CH61-79,  $S_w^0 = .1517$  with the measured value of  $K'$  increasing in the 105 kHz data from a dry value of 6.07 to a wetted value of 28.68. In the data for Berea 100,  $S_w^0 = .1100$  with  $K'$  increasing in the 105 kHz data from a dry value of 5.7 to a wetted value of 12.9.

As discussed above, it is obvious that geometrical and surface effects must be taken into account when modeling  $K'$

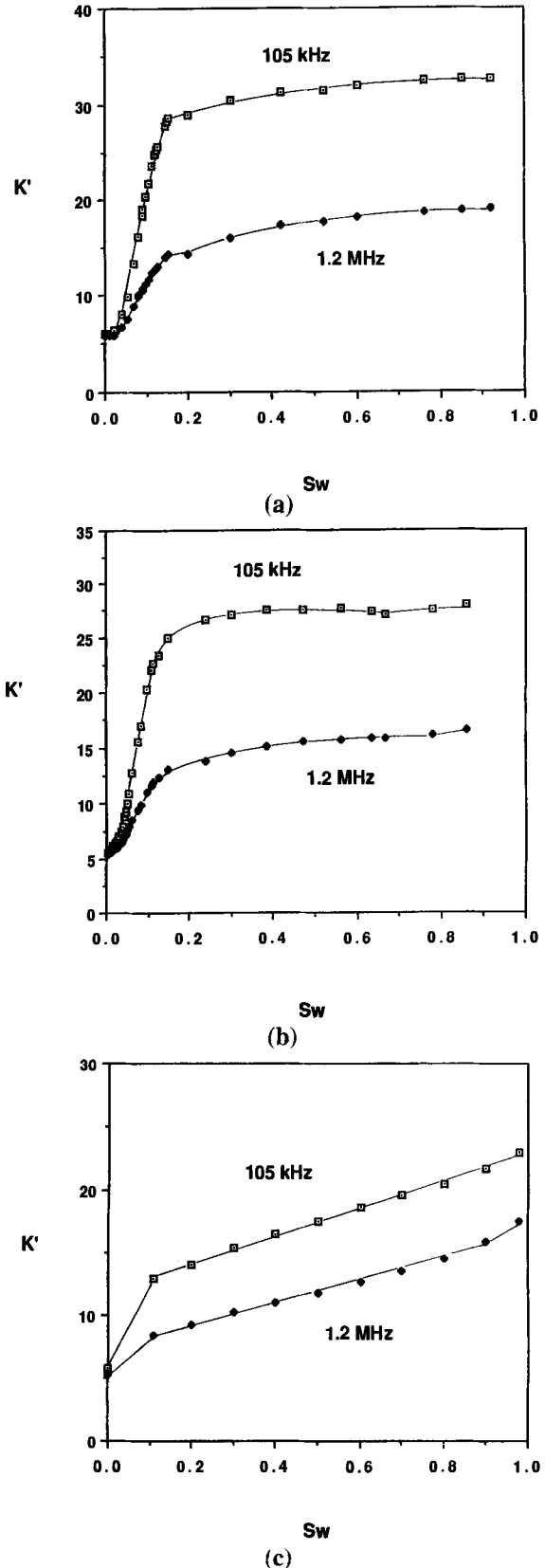


FIG. 1.  $K'$  versus  $S_w$  for the three sandstones at two frequencies, 105 kHz and 1.2 MHz. (a) CH61-79, (b) CH58-79, (c) Berea 100.

of a rock-water mixture. What we are suggesting, based upon these data, is that geometrical and surface effects associated with water-saturated rocks, and the related frequency dispersion, are all established within the low saturation region ( $S_w < S_w^0$ ). We propose using  $K'$  measured at  $S_w^0$  as a starting point for modeling the dielectric response of a rock as a function of water saturation. By using the dielectric value of the wetted rock, instead of the dry rock as is usually done, we are considering a system in which the components, rock and water, have come to equilibrium. Geometrical and surface effects are included in  $K'$  measured at  $S_w^0$ , so they need not be included in the theoretical model; therefore, we can use existing models. We believe defining the basic components in this way is a more reasonable starting point for theoretically modeling dielectric data.

#### EFFECTIVE MEDIUM THEORY

We selected the three-component effective medium theory (EMT) of Feng and Sen (1985) to model our data. Their

analytic solution was used and solved by means of the Newton-Raphson method. When we use the effective medium theory with the dielectric constants and volume fractions of the dry rock and the water as input parameters, the theory does not fit the data. The results for the CH61-79 data at 105 kHz are shown in Figure 3a, and for 1.2 MHz in Figure 3b. It is quite obvious that by using  $K'$  of the dry rock, the measured  $K'$  of the rock-water system cannot be predicted using the effective medium theory in this way. It is also clear from these figures that the theory parallels the change in  $K'$  with  $S_w$  and is only in error due to the large increase in  $K'$  at low saturations that cannot be modeled with the effective medium theory in its present form.

We next redefine our system as composed of the three components: the wetted rock (which is the dry rock coated with the surface water), the bulk water in the pore space (which excludes the surface water), and the air which occupies the remainder of the pore space at any given  $S_w$ . We maintain the assumption at this stage that the dielectric

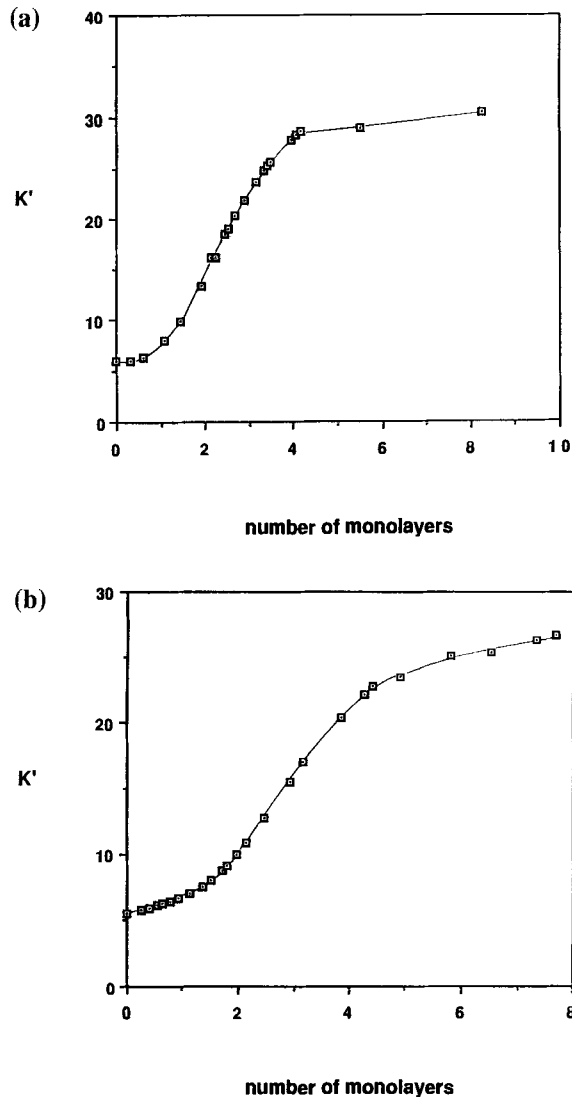


FIG. 2.  $K'$  versus number of completed monolayers for two samples. (a) CH61-79, (b) CH58-79. The data were collected at a frequency of 105 kHz.

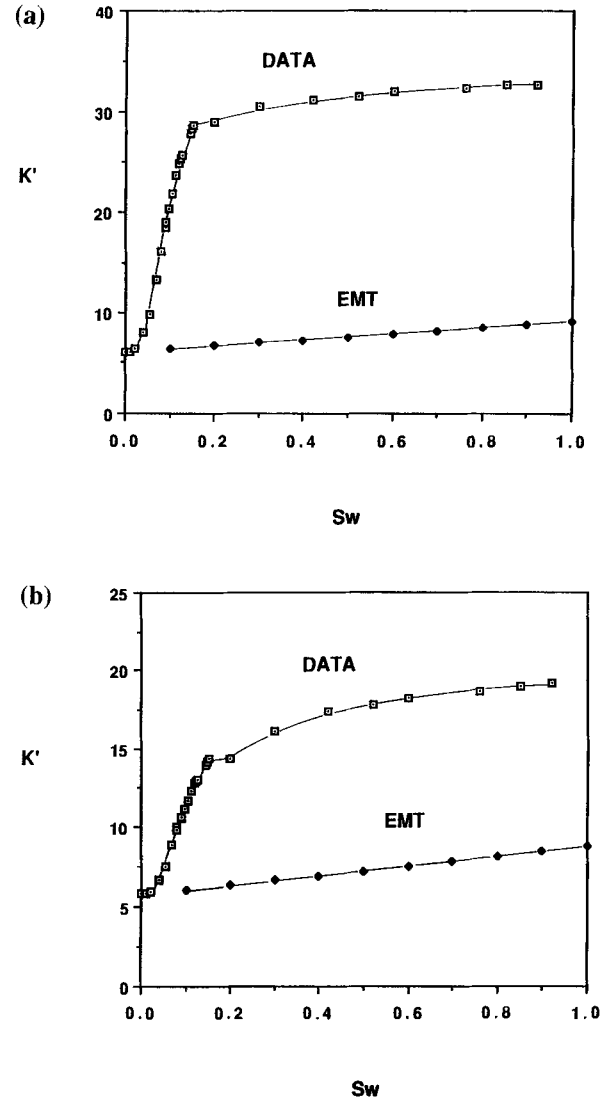


FIG. 3. Comparison of data from sample CH61-79 with effective medium theory (EMT). (a) Frequency equals 105 kHz; (b) Frequency equals 1.2 MHz.

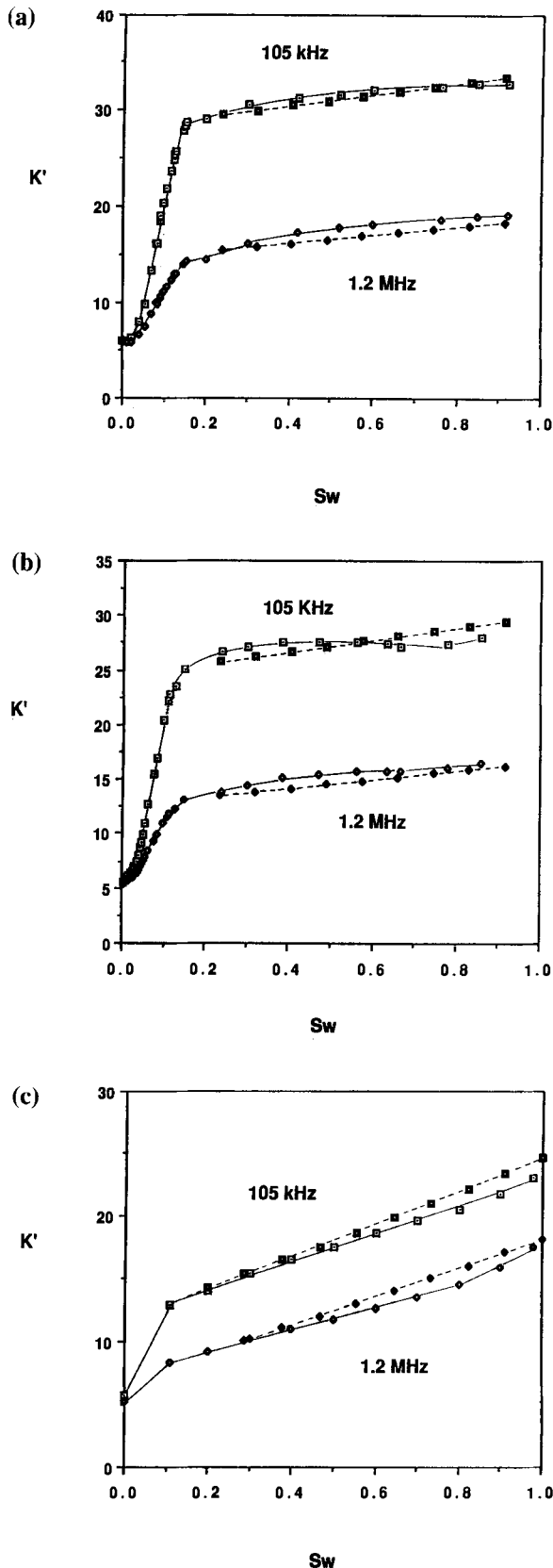


FIG. 4. Comparison of data for the three sandstones with effective medium theory for the wetted rock, bulk water, air system. Data are open symbols connected with a solid line; effective medium theory results are solid symbols connected with a broken line. (a) CH61-79; (b) CH58-79; (c) Berea 100.

Table 2. Input parameters for the model.

Sample	$S_w^0$	$\Phi_c$	$K'_{wr}$	
			105 KHz	1.2 MHz
CH61-79	.1517	.0594	31.70	15.73
CH58-79	.1496	.0587	27.68	14.30
Berea 100	.1100	.175	17.19	10.77

constants of both the rock and the air are real. A portion of the total porosity of the rock ( $\phi_t$ ) is filled by the surface water, so we define a surface water-filled porosity ( $\phi_s$ ):

$$\phi_s = S_w^0 \phi_t$$

and define a corrected porosity ( $\phi_c$ ) as the porosity available for filling with bulk water

$$\phi_c = \phi_t - \phi_s.$$

In rocks with small surface-area-to-volume ratios, this is a minor correction, but in samples with surface-area-to-volume ratios on the order of  $10^6 \text{ cm}^{-1}$  (such as samples CH58-79 and CH61-79), approximately 15 percent of the pore space is filled with surface water.

The level of water saturation in a rock is usually defined as the volume fraction of the total available pore space filled with water:

$$S_w = \frac{V_w}{V_p},$$

where  $V_w$  is the total volume of water present (surface and bulk water) and  $V_p$  is the total volume of the pore space. In our system we define a corrected  $S_w$  ( $S_{wc}$ ) as the volume fraction of the corrected pore space volume ( $V_{pc}$ ) (excluding the volume occupied by surface water) filled with bulk water

$$S_{wc} = \frac{V_{bw}}{V_{pc}},$$

where  $V_{bw}$  is the volume of bulk water only.  $S_{wc}$  is related to  $S_w$  by the expression

$$S_w = S_{wc}(1 - S_w^0) + S_w^0.$$

The volume fractions of our components, wetted rock ( $wr$ ), bulk water ( $bw$ ), and air ( $g$ ) become

$$V_{wr} = (1 - \phi_c),$$

$$V_{bw} = S_{wc} \phi_c,$$

and

$$V_g = (1 - S_{wc}) \phi_c.$$

The results of modeling the data using the effective medium theory for the wetted rock-water system are shown in Figures 4a to 4c. The input parameters for each sample and frequency are given in Table 2. The water used in the experiments was deionized water;  $K'_w = 80$ ,  $K''_w = 8.25$  at 105 kHz, and  $K''_w = .225$  at 4 MHz. For the air,  $K'_a = 1.01$ . By starting with the wetted system, such that our model

applies in the range  $S_w^0 < S_w < 1.0$ , we find very good agreement with the theory.

CRIM

We next consider using CRIM as a model for  $K'$  of a partially saturated rock. When CRIM is used in its original form, using the dielectric constants and volume fractions of the dry rock, water, and air, there is poor agreement with the data. This is shown in Figures 5a and 5b, where the data from CH61-79 at 105 kHz and 1.2 MHz are compared with the CRIM model.

We can rewrite the CRIM equation for a partially saturated rock defined as being composed of wetted rock, bulk water, and air using our corrected parameters as defined above:

$$\sqrt{K^*} = (1 - \phi_c)\sqrt{K'_{wr}} + S_{wc}\phi_c\sqrt{K^*_{bw}} + (1 - S_{wc})\phi_c\sqrt{K'_a}$$

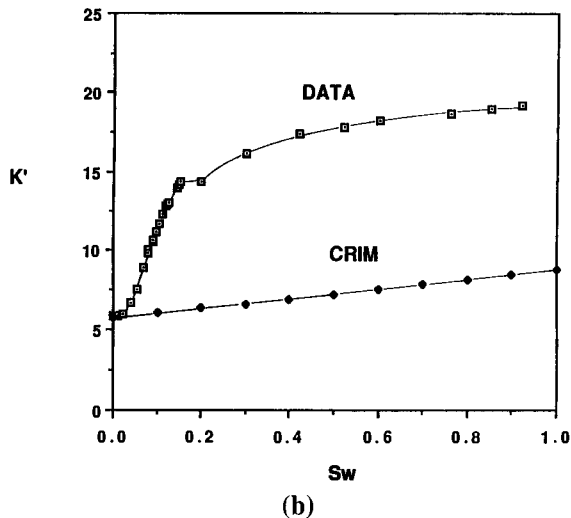
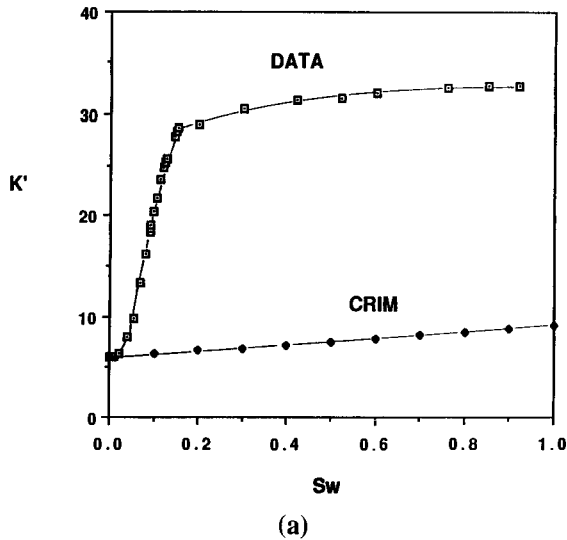


FIG. 5. Comparison of data from sample CH61-79 with CRIM. (a) Frequency equals to 105 kHz; (b) frequency equals 1.2 MHz.

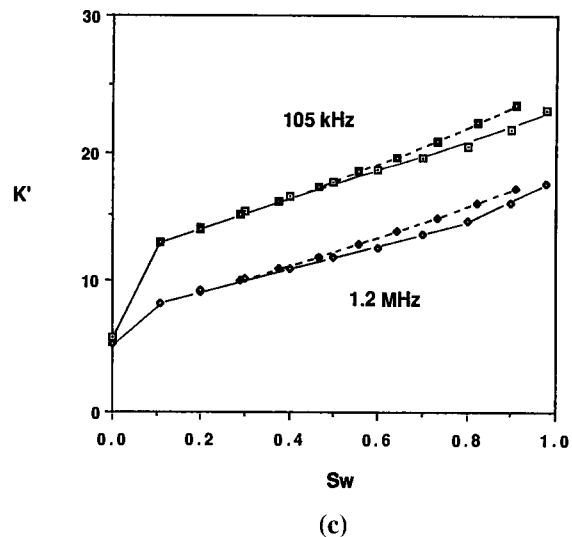
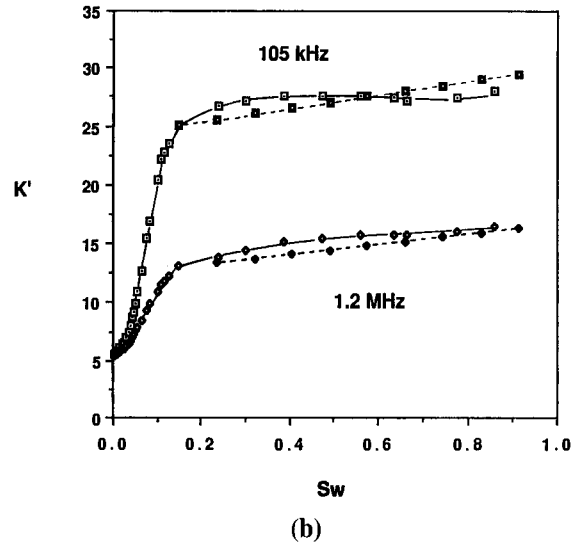
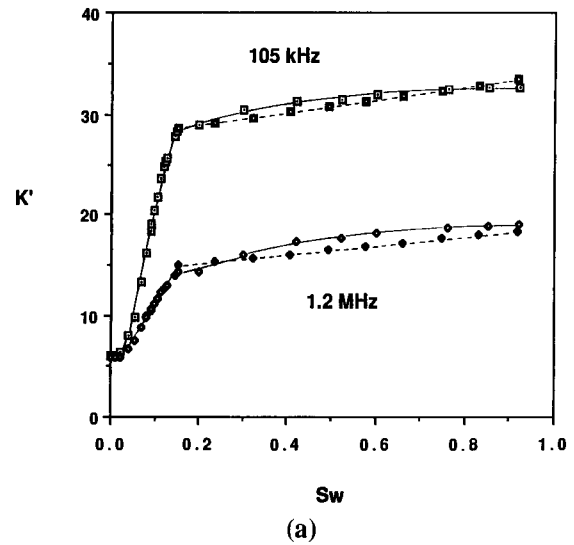


FIG. 6. Comparison of data for the three sandstones with CRIM for the wetted rock, bulk water, air system. Data are open symbols connected with a solid line; CRIM results are solid symbols connected with a broken line. (a) CH61-79; (b) CH58-79; (c) Berea 100.

or, in terms of  $S_w$  and  $\phi_t$ ,

$$\sqrt{K^*} = [1 - \phi_t(1 - S_w^0)]\sqrt{K'_{wr}} + (S_w - S_w^0)\phi_t\sqrt{K'_{bw}} + (1 - S_w)\phi_t\sqrt{K'_a}$$

When CRIM in this form is applied to our data to model  $K'$ , using the input parameters listed in Table 2, we again find very good agreement with our data. The experimental data and the results of modeling with CRIM are shown in Figures 6a, 6b, and 6c. As can be seen, the results we obtained using CRIM are essentially identical to those obtained for the effective medium theory. This was expected, because for low-salinity water which results in a small value for  $K''$ , the effective medium theory and CRIM have been found to show good agreement (Feng and Sen, 1985).

### COMPLEX MATRIX PARAMETERS

We have found that using  $K'$  of the wetted rock, measured at  $S_w^0$ , greatly improves the agreement between existing models and our data. In both the three-component effective medium theory and CRIM, the matrix has been defined as having a totally real dielectric constant because it was assumed that the matrix was nonconducting. If we look at the conductivity data for the studied samples, however, it is obvious that the adsorption of the surface water increases the conductivity of the system by two to three orders of magnitude. This can be seen in Figure 7, where the conductivity of sample CH61-79 measured at 105 kHz is plotted as a function of  $S_w$ . The increased conductivity between the dry and wetted state makes it unreasonable in our treatment to assume a nonconducting rock matrix. To allow for a conducting rock matrix, the conductivity of the matrix of each sample was determined from the measured data at  $S_w^0$  and was used to calculate an imaginary component  $K''$  for the dielectric constant of the wetted rock.

In the case of the CRIM model, the equation becomes

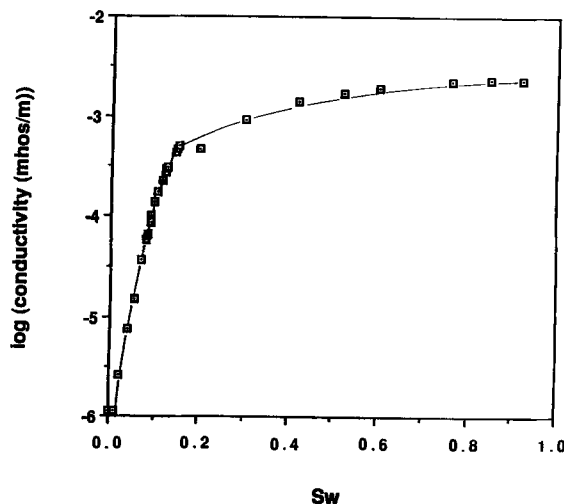


FIG. 7. Log (conductivity) versus  $S_w$  measured for CH61-79 at 105 kHz.

$$\sqrt{dK^*} = (1 - \phi_c)\sqrt{K'_{wr}} + S_{wc}\phi_c\sqrt{K'_{bw}} + (1 - S_{wc})\phi_c\sqrt{K'_a}$$

where  $K_{wr}^*$  is now the complex dielectric constant of the rock matrix. The differential form of the effective medium theory of Feng and Sen becomes

$$\frac{dK^*}{3K^*} = \frac{dV_m}{V_m + V_w + V_n} \frac{K_m^* - K^*}{K_m^* + 2K^*} + \frac{dV_n}{V_m + V_w + V_n} \frac{K'_n - K^*}{K'_n + 2K^*}$$

This has an analytic expression for the solution of the initial value problem similar in form to the one found by Feng and Sen for the original problem of a nonconducting rock matrix. However, in the case of complex dielectric constants for the rock matrix, we found that the Newton-Raphson method had convergence difficulties, so we solved the differential equation directly by use of a Runge-Kutta-Fehlberg method. As before, volume fractions were corrected to include the adsorbed surface water as part of the rock matrix.

The results from the effective medium theory when complex matrix parameters are used are shown in Figure 8a for CH61-79 and in Figure 8b for Berea 100; the results from CRIM are shown in Figure 9a for CH61-79 and in Figure 9b for Berea 100. Again the results using CRIM are practically identical to those for the effective medium theory. We found that including a conductivity term for the rock matrix had no effect on the results at 1.2 MHz. At 105 kHz, however, treating the rock matrix as complex resulted in an overestimation of  $K'$  of the partially saturated rock at the high levels of water saturation. This effect was more pronounced in the high-porosity sandstone, Berea 100.

### CONCLUSIONS

Existing theoretical models to predict the dielectric response of rock-water mixtures use the volume fractions and dielectric constants of the dry rock matrix and the water as input parameters. The discrepancy between measured and theoretically predicted  $K'$  for saturated rocks obtained when using these models has been attributed to geometrical and electrochemical effects in saturated rocks that are unaccounted for in the theories. We have found that the use of wetted matrix parameters provides excellent agreement between theory and data. We suggest, based on these observations, that all geometrical and electrochemical effects in saturated rocks are in fact associated with the interaction at the rock-water interface; once the rock-water interface has been fully established through the adsorption of approximately 1 nm of water, the magnitudes of all geometrical and electrochemical effects have been established. Starting with wetted matrix parameters thus includes all geometrical and electrochemical effects and makes it possible to use existing theories to model the data.

We have found the best agreement between theory and data when the matrix was treated as wetted but nonconducting. The large increase in conductivity associated with the wetting of the rock matrix shows quite clearly that the wetted matrix should be treated as conducting, but our

attempts to include a matrix conductivity have been unsuccessful. The main problem appears to be in determining the conductivity value that should be assigned to the wetted matrix given the interaction between surface conductivity and bulk conductivity that occurs as  $S_w$  increases.

While we have been successful in modeling our laboratory data, two issues need to be addressed in order to assess the applicability of these results to the interpretation of borehole dielectric measurements: the frequency range, and the nature and distribution of the pore fluids.

Frequency clearly has a large effect on the wetted matrix parameters. As frequency increases, the magnitude of the surface effect decreases, such that by 4 MHz in the sandstone data presented here  $K'_{wr}$  is approaching  $K'_{dry\ rock}$ . The question should be asked whether the use of wetted matrix parameters is unnecessary at frequencies above 10 MHz. Their use depends upon the specific mechanism and the conductivity. Kenyon (1984) has described a scaling of

frequency with conductivity for geometrical effects in water-saturated rocks. If the surface water effect is predominantly a geometrical effect, this scaling is such that the effects we observe at 105 kHz with deionized water would exist at 1 GHz in rocks saturated with a solution of conductivity of 0.5 mhos/m. The use of wetted matrix parameters in interpretation models could therefore be very important in the frequency range commonly used in making borehole dielectric measurements.

In the data considered here, the pore space contained water and air. We have attributed the large increase in  $K'$  at low saturations, which led to our defining the parameter  $K'_{wr}$ , to the presence of water coating the surface of the pore space; i.e., water is the wetting fluid. If oil were the second fluid phase in the pore space, instead of air, we would thus expect the same  $K'$ -versus- $S_w$  behavior as long as the sandstone remained water-wet. In an oil-wet system, it is unclear what would occur at low saturations; the question is a topic that requires further study.

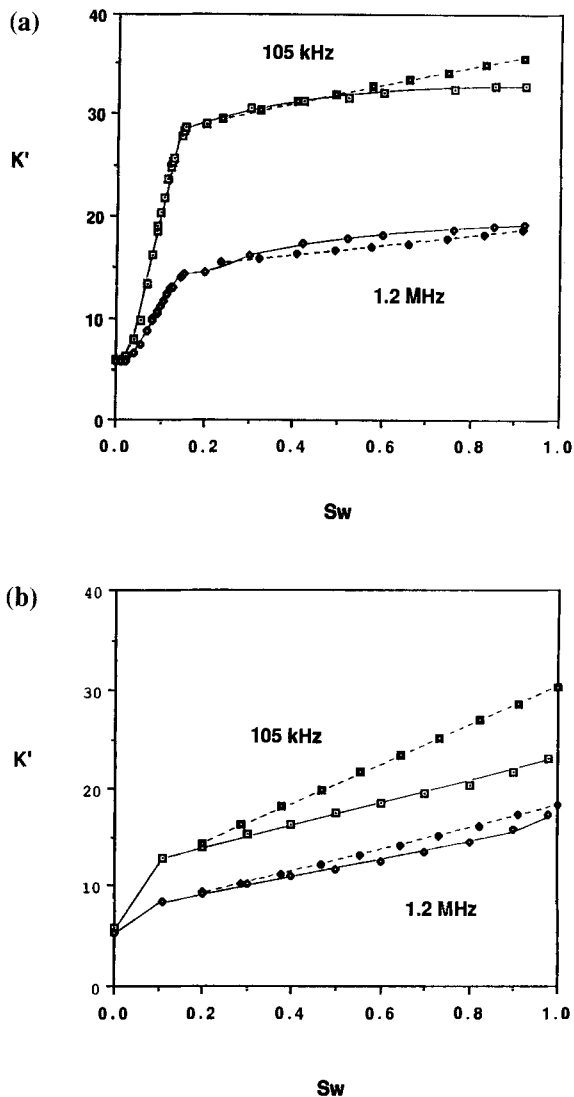


FIG. 8. Comparison of data with results from effective medium theory when a complex matrix dielectric constant is used. Data are open symbols connected with a solid line; effective medium theory results are solid symbols connected with a broken line. (a) CH61-79; (b) Berea 100.

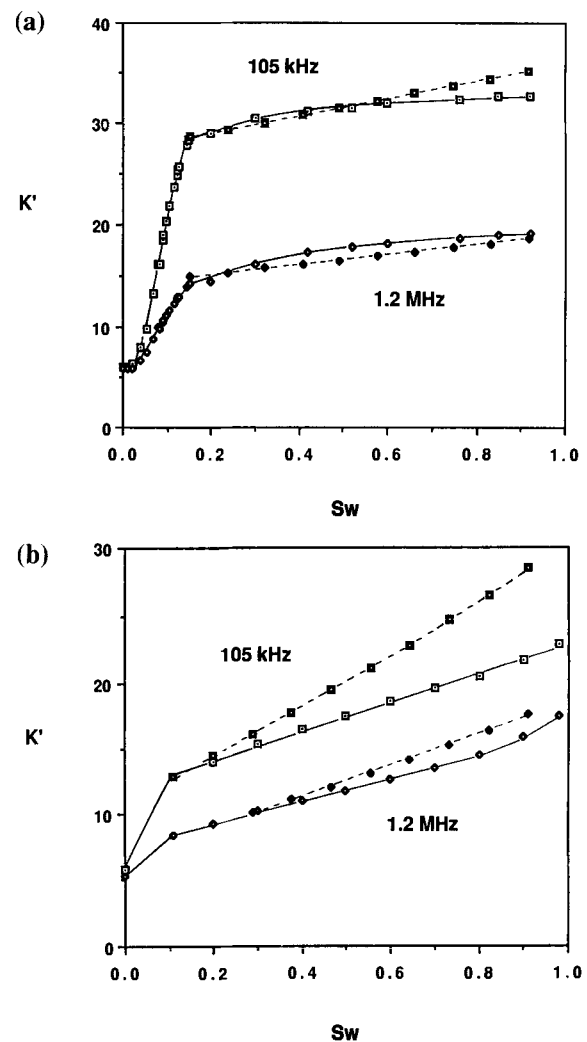


FIG. 9. Comparison of data with results from CRIM when a complex matrix dielectric constant is used. Data are open symbols connected with a solid line; CRIM results are solid symbols connected with a broken line. (a) CH61-79; (b) Berea 100.



An additional complication in the interpretation of dielectric data is the observation that the saturation history of a rock, and the resulting microscopic fluid distribution, can affect the form of  $K'$  versus  $S_w$  at the higher levels of saturation,  $S_w > S_w^0$  (Knight and Nur, 1987b). This is an additional geometrical effect that needs to be modeled and cannot be accounted for with the existing theories. It is interesting to note, however, that regardless of the fluid distribution and the corresponding effects on  $K'$  in the region  $S_w > S_w^0$ , the behavior of the rock-water system in the region  $0 < S_w < S_w^0$  remains the same. Thus, we conclude that the basic component in theoretically modeling the dielectric response of water-wet rocks, whatever the composition or geometry of the contained pore fluids, must be the wetted matrix dielectric values.

#### REFERENCES

- Feng, S., and P. N. Sen, 1985, Geometrical model of conductive and dielectric properties of partially saturated rocks: *J. Appl. Phys.*, **58**, 3236–3243.
- Fuller, B. D., and Ward, S. H., 1970, Linear system description of the electrical parameters of rocks: *IEEE Trans. on Geosci. Electron.*, **GE-8**, 7–18.
- Gassmann, F., 1951, Uber die elastizitat poroser medien: *Vierteljahrsschr. Naturforsch. Ges. Zurich*, **96**, 1–21.
- Keller, G. V., and Licastro, P. H., 1959, Dielectric constant and electrical resistivity of natural state cores: *U.S. Geol. Surv. Bull.*, **1052-H**, 257–285.
- Kenyon, W. E., 1984, Texture effects on megahertz dielectric properties of calcite rock samples: *J. Appl. Phys.*, **55**, 3153–3159.
- Knight, R. J., and A. Nur, 1987a, The dielectric constant of sandstones, 60 kHz to 4 MHz: *Geophysics*, **52**, 644–654.
- , 1987b, Geometrical effects in the dielectric response of partially saturated sandstones: *The Log Analyst*, **28**, 513–519.
- Lysne, P. C., 1983, A model for the high-frequency electrical response of wet rocks: *Geophysics*, **48**, 775–786.
- Norris, A. N., Callegari, A. J., and Sheng, P., 1985, A generalized differential effective medium theory: *J. Mech. Phys. Solids*, **33**, 525–543.
- Sen, P., 1980, The dielectric and conductivity response of sedimentary rocks: *Soc. of Petr. Eng. AIME*, paper 9379.
- Sherman, M. M., 1987, A model for the determination of water saturation from dielectric permittivity measurements: *The Log Analyst*, **28**, 282–288.
- Thorp, J. M., 1959, The dielectric behavior of vapours adsorbed on porous solids: *Trans. Faraday Society*, **55**, 442–454.
- Wharton, R. P., G. A. Hazen, R. N. Rau, and D. L. Best, 1980, Electromagnetic propagation logging: advances in technique and interpretation: *Soc. Petr. Eng., AIME*, paper 9267.